Active screen plasma nitriding enhances cell attachment to polymer surfaces

Journal Item

Active screen plasma nitriding enhances cell attachment to polymer surfaces

Georgia Kaklamani[1*], James Bowen[2], Nazia Mehrban[2], Hanshan Dong[1], Liam M Grover[2] and Artemis Stamboulis[1]

[1]University of Birmingham, College of Engineering and Physical Sciences, School of Metallurgy and Materials, Edgbaston, Birmingham B15 2TT, UK
[2]University of Birmingham, College of Engineering and Physical Sciences, School of Chemical Engineering, Edgbaston, Birmingham B15 2TT, UK

*Corresponding author:
Tel.: +44 (0) 121 414 5357;
Fax: +44 (0) 121 414 5397;
E-mail: g.kaklamani@bham.ac.uk

Abstract

Active Screen Plasma Nitriding (ASPN) is a well-established technique used for the surface modification of materials, the result of which is often a product with enhanced functional performance. Here we report the modification of the chemical and mechanical properties of ultra-high molecular weight poly(ethylene) (UHMWPE) using 80:20 (v/v) N_2/H_2 ASPN, followed by growth of 3T3 fibroblasts on the treated and untreated polymer surfaces. ASPN-treated UHMWPE showed extensive fibroblast attachment within three hours of seeding, whereas fibroblasts did not successfully attach to untreated UHMWPE. Fibroblast-coated surfaces were maintained for up to 28 days, monitoring their metabolic activity and morphology throughout. The chemical properties of the ASPN-treated UHMWPE surface were studied using X-ray photoelectron spectroscopy, revealing the presence of C-N, C=N, and C≡N chemical bonds. The elastic modulus, surface topography, and adhesion properties of the ASPN-treated UHMWPE surface were studied over 28 days during sample storage under ambient conditions and during immersion in two commonly used cell culture media.

Keywords

Active screen plasma nitriding, atomic force microscopy, fibroblast, interferometry, nanoindentation, X-ray photoelectron spectroscopy

1. Introduction

Biomaterials that will be used for medical applications are required to have excellent bulk and surface properties to resist mechanical deformation while providing a surface that enables tissue attachment. Designing a material that exhibits good bulk properties together with the appropriate surface characteristics to enable biological integration is often challenging [1-3]. Polymeric materials exhibit attractive characteristics for biomedical applications. They are of low density, are easy to process and of relatively low cost. It has also been reported that polymers can be tailored to influence the viability, growth and function of attached cells controlling the cell function by the chemical, morphological and mechanical properties of the polymeric surface [4]. The surface properties of polymers, however, do not often satisfy the requirements for biomedical applications such as scratch resistance, wettability, biocompatibility, gas permeability and friction. They often appear to have low surface energy and poor adhesive properties hence surface modification is required [5-8].

Plasma surface modification (PSM) has been widely used to modify the surface properties of polymeric materials [9]. For biomaterials in particular, the plasma method has proved to be effective in altering surface characteristics while maintaining the bulk properties of the material [10-13]. One of the major advantages of PSM is the enhancement of the material's biological reactivity [2]. Other surface characteristics that can be improved by PSM are wettability, refractive index, chemical inertness, hardness and lubricity, by introducing new functional groups depending on the gas used (e.g. O_2, N_2) [14-15]. N_2-containing plasmas are often used to modify the surface of polymers due to their ability to incorporate functionalities such as amine moieties on the surface structure of materials [7-8]. However, the exact nature of the plasma modified polymeric surface is difficult to identify. This is due to the complexity of its chemistry and the small thickness of the film, typically a few nanometres.

There are numerous drawbacks associated with the conventional direct current (DC) plasma PSM technique, such as non-uniformity of plasma temperature during treatment, arcing, edging and the hollow cathode effect, all of which can damage the samples. The Active Screen Plasma Nitriding (ASPN) technique was first reported in 1999 as a method which avoided the drawbacks associated with PSM [16]. The main advantage of the ASPN technique is the capacity to homogeneously treat surfaces of any morphology. To date ASPN has been applied to metals such as low alloy steel, copper and austenitic stainless steel in order to achieve hardening [17-20].

Ultra-high molecular weight poly(ethylene) (UHMWPE) has a long history as a successful biomaterial and is frequently used in total joint replacements. As such, it is a relevant choice of model polymer for the assessment of the usefulness of ASPN to improve the biocompatibility of implantable polymers. Previously we reported the results of a feasibility study regarding the effect of ASPN on UHMWPE surfaces [21] in which the modification was shown to be successful. In the work presented here, we investigate the mechanical, chemical and topographical properties of the ASPN-treated UHMWPE surface as a function of treatment time, and also as a function of storage environment and storage time. Samples were stored for up to 28 days under (i) air, (ii) phosphate buffered saline, and (iii) Dulbecco's Modified Eagle Medium supplemented with foetal bovine serum. It is anticipated these tests will provide useful information regarding the stability of the ASPN treatment upon immersion in aqueous environments commonly used for cell culture. Finally, we report on the attachment, morphology, and metabolic activity of 3T3 fibroblasts seeded on the ASPN-treated UHMWPE surface over a period of 28 days.

2. Materials and Methods

2.1 UHMWPE

UHMWPE was supplied in the form of a pressed and planed flat sheet with dimensions 201 x 297 x 20 mm^3 (Oadby Plastics, UK). The average surface roughness, S_a, of the sheet as received was measured using interferometry and was found to be 720 ± 100 nm. The molecular weight of the polymer was $9.2x10^6$ g/mol. In order to prepare the UHMWPE samples for ASPN treatment, square pieces of 15 x 15 x 2 mm^3 UHMWPE were cut. Prior to ASPN treatment, all samples were washed with distilled H_2O and EtOH (HPLC grade, Fisher Scientific, UK) and were left to dry in air at 20 ^oC.

2.2 ASPN treatment

Surface modification of UHMWPE was performed using ASPN, which consisted of a conventional 40 kW DC nitriding furnace (Klockner Ionan) together with an active screen (AS) experimental arrangement. The AS was set inside the nitriding furnace and around the workload. The AS was made of 700 µm thick perforated (AISI 304) sheet steel, with a height of 130 mm, a diameter of 120 mm and with holes of 8 mm in diameter. The sample-to-AS distance was 10 mm. A schematic of the ASPN system is shown in Fig. 1. A high voltage cathodic potential was applied on the screen, whilst the working table was electrically insulated with ceramic spacers, thus leaving the specimens at a floating potential. The typical values of voltage and current were 250 V and 1 A respectively. The furnace walls were on an anodic potential. The samples and the working table were insulated from the cathodic potential (screen) and anodic potential (furnace wall). The gas mixture in the plasma chamber was 80 % N_2 and 20 % H_2 (v/v); the chamber pressure was 2.5 mbar and the treatment temperature was 90 ^oC. UHMWPE samples were ASPN treated for 10, 30 and 60 mins (ASPN10, ASPN30 and ASPN60). Samples were placed in a vacuum desiccator and stored at a pressure of 10^{-2} mbar immediately following treatment. Samples were transferred within 1 h of manufacture to one of the three different storage environments outlined in §2.4.

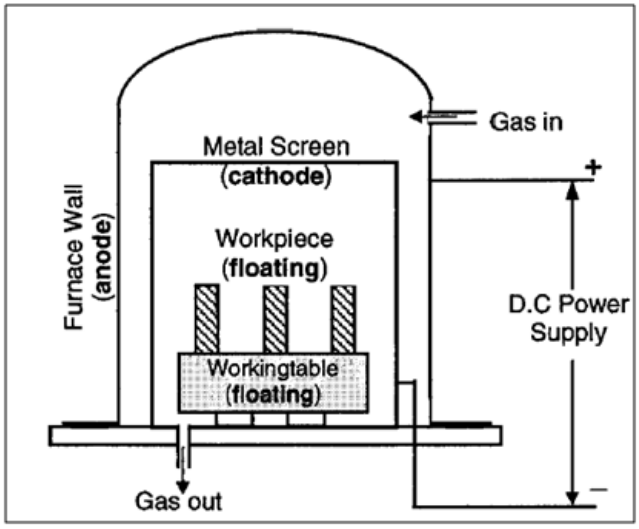

Figure 1. Schematic of the Active Screen Plasma Nitriding surface modification method [17].

2.3 Physicochemical characterization of UHMWPE

2.3.1 Surface composition

The composition and surface chemical bonds of treated and untreated UHMWPE surfaces were investigated using X-ray photoelectron spectroscopy (XPS); ASPN-treated samples were measured within 24 h of treatment. Analysis was

performed using a VG Escalab 250 XPS, operating a monochromated Al Kα X-ray source, with a spot size of 500 nm and a power of 150 W. The step size in order to obtain individual peaks was 0.1 eV, whereas 1 eV was used for the acquisition of a full spectrum over the complete range of binding energies. The vacuum pressure in the analysis chamber was < 10^{-9} mbar. All high resolution spectra were deconvoluted using the XPSPEAK41 software. The C 1s (285 eV binding energy), N 1s (400 eV binding energy) and O 1s (531 eV binding energy) photoelectron peaks were analysed in detail. Data were fitted using the Gauss-Lorentz function, and the Shirley method was used for background subtraction.

2.3.2 Surface topography

Interferometry was employed to evaluate the topography and roughness of UHMWPE surfaces before and after ASPN treatment. Measurements were performed using a MicroXAM2 interferometer (Scantron, UK), operating using a white light source. Samples were imaged using a 10X objective lens, which corresponded to an analysis window of dimensions 864 x 642 μm^2. Scanning Probe Image Processor software (Image Metrology, Denmark) was employed for the analysis of acquired images, yielding S_a, S_q and S_z values for surface roughness, each of which were the mean of a minimum of five measurements at separate locations.

2.3.3 Mechanical properties

The hardness and reduced modulus of the UHMWPE surface were obtained by performing indentation measurements to a depth of 500 nm using a NanoTest (Micro Materials, UK) employing a diamond-coated Berkovich indenter. A minimum of 30 measurements were performed over various locations of the sample surface.

2.3.4 Adhesive properties

Acquisition of adhesion data was performed using a NanoWizard II AFM (JPK Instruments, UK) employing a CellHesion module (JPK Instruments, UK), operating in contact mode at 18 ^oC and 40 % relative humidity. A minimum of 25 adhesion force measurements were performed, employing rectangular 130 µm length Si cantilevers with 6 µm nominal radius SiO_2 colloid probes at their apex (NovaScan, USA). Cantilever spring constants were on the order of 25-30 N/m, as calibrated according to the method reported by Bowen *et al.* [22].

2.4 Stability study

The stability of the ASPN treatment on the UHMWPE sample surfaces was assessed over 28 days post-treatment, exposing the samples to three commonly encountered environmental conditions. Immediately after treatment, samples were sterilised with 70:30 EtOH:H_2O and were immobilised in poly(styrene) 12 well-plates of diameter 22 mm and height 20 mm (Scientific Laboratory Supplies, UK) using double-sided carbon tape (Agar Scientific, UK) on their undersides. The storage environments chosen were (i) air, (ii) 2 mL phosphate buffered saline (PBS, Sigma Aldrich, UK), and (iii) 2 mL Dulbecco's Modified Eagle's Medium (DMEM, Sigma Aldrich, UK) supplemented with 10 % v/v foetal bovine serum (FBS, PAA, Germany). The supplemented DMEM is abbreviated as S-DMEM throughout the remainder of this work. All samples were placed in an incubator (MCO-15AC, Sanyo Electric Co. Ltd., UK) at a temperature of 37 °C and in a 5 % v/v CO_2 atmosphere at 100 % RH for up to 28 days. The topography, adhesive properties, mechanical properties and composition of the surface of ASPN-treated samples were measured on Days 0, 7, 14 and 28. Day 0 corresponds to 3 h post-treatment. One sample was used for each day/environment combination, and there was no re-use of samples following removal from storage.

2.5 Fibroblast culture

NIH 3T3 fibroblasts (LGC, UK) were used to study the cellular compatibility of the ASPN-treated UHMWPE surfaces. Fibroblasts were cultured in T175 tissue culture flasks (Sarstedt, UK) in S-DMEM which was further supplemented with 2.4 % v/v L-glutamine, 2.4 % v/v 4-(2-hydroxyethyl)-1-piperazineethanesulfonic acid (HEPES) buffer and 1 % v/v penicillin/streptomycin. PBS was used to wash fibroblasts before seeding on the plasma treated and untreated surfaces. Fibroblasts were passaged using trypsin on the 7th day after culture in S-DMEM. To determine the concentration of viable fibroblasts in the suspension, 1 mL was removed from the flask and the fibroblasts therein were stained with trypan blue and counted using a haemocytometer (Sigma-Aldrich, UK) under a light microscope (Olympus, UK).

2.6 Surface seeding

ASPN-treated and untreated UHMWPE samples were sterilised under UV light for 12 h prior to seeding. Samples were subsequently immobilised in poly(styrene) 12 well-plates of diameter 22 mm and height 20 mm (Scientific Laboratory Supplies, UK) using double-sided carbon tape (Agar Scientific, UK) on their undersides. Fibroblast suspension in S-DMEM was added to each well at a seeding density of $1.2x10^6$ fibroblasts per sample. The fibroblast-seeded surfaces were replenished with an additional 2 mL S-DMEM and placed in an incubator (MCO-15AC, Sanyo Electric Co. Ltd., UK) at a temperature of 37 °C and in a 5 % v/v CO_2 atmosphere at 100 % RH for up to 28 days. The S-DMEM in each well was replenished every 3 days. All chemicals for cellular studies were purchased from Sigma-Aldrich, UK

2.7 Characterization of fibroblast-seeded UHMWPE

2.7.1 Scanning electron microscopy

Fibroblast-seeded samples were visualised using scanning electron microscopy (SEM; JSM 6060 LV, JEOL, Oxford Instruments, UK). The operating voltage was 10 kV, the working distance was 10 mm and the spot size was 3. Prior to analysis, samples were chemically fixed using 2.5 % v/v aqueous glutaraldehyde solution (Sigma-Aldrich, UK) for 24 h and dehydrated using EtOH (HPLC grade, Fisher Scientific, UK). Afterwards, the samples were washed in 70:30, 90:10 and 100:0 EtOH:H_2O solutions for 30 min followed by anhydrous EtOH for an additional 30 min. The samples were then critical point dried via immersion in liquid CO_2 at 1,070 psi at 31 ^oC for 60 min. Finally, the specimens were Pt coated using a SC7640 sputter coater (Polaron, UK); the thickness of sputtered Pt film was in the range 10-12 nm. SEM imaging was performed for all treated (ASPN10, ASPN30, and ASPN60) and untreated samples 24 h after seeding. SEM imaging was also performed for ASPN60 only on Day 14 and Day 28 after seeding.

2.7.2 Surface topography

Interferometry was employed to evaluate the topography of fibroblast-seeded sample surfaces. Measurements were performed using a MicroXAM2 interferometer (Scantron, UK), operating using a white light source. Samples were imaged using a 20X objective lens, which corresponded to an analysis window of dimensions 432 x 321 μm^2. The purpose of these measurements was to assess cellular morphology and to measure the thickness of the fibroblast layer formed on the sample surface. Measurements were performed for ASPN60 only on Days 0, 7, 14, and 28 after seeding.

2.7.3 Atomic force microscopy

ASPN60 samples were tested on Days 0, 7, 14 and 28 after seeding. Acquisition of topographical and adhesion data was performed using a NanoWizard II AFM (JPK Instruments, UK) employing a CellHesion module (JPK Instruments, UK), operating in force scan mapping mode at 18 ^oC. The sample and cantilever were immersed in S-DMEM,

contained within a clean glass Petri dish. Rectangular 130 µm length Si cantilevers (type NSC36/no Al, Mikro Masch, Estonia) having pyramidal tips with 10 nm nominal radii of curvature were used; cantilever spring constants were on the order 0.2 N/m and were calibrated according to the method reported by Bowen *et al.* [22]. Data were acquired by driving the fixed end of the cantilever at a velocity of 50 µm/s towards the sample surface, whilst monitoring the deflection of the free end of the cantilever. Upon making contact with a surface feature, the height of the contact point was recorded, representing one pixel in the image, which was converted into a map of surface topography. Force curves acquired on fibroblasts were analysed in order to assess the adhesion properties of the surface. A maximum compressive load of 5 nN was applied to the surface during data acquisition, which corresponded to a small strain during the indentation of a fibroblast.

2.7.4 Metabolic activity assay

In order to quantify the approximate number of viable cells on the surface of ASPN60, a tetrazolium assay was performed on Days 0, 7, 14 and 28. This colorimetric assay uses the metabolic activity of enzymes from viable cells present in the reaction mixture to convert the tetrazolium dye to formazan, an insoluble crystal with a distinctive purple colour. Briefly, 200 µL yellow MTT (3-(4, 5-Dimethylthiazol-2-yl)-2,5-diphenyltetrazolium bromide) solution was added to each sample and incubated at 37°C under conditions of 5 % v/v CO_2 and 100 % relative humidity for 18 h. The incubation allows the tetrazolium ring in the salt to cleave under the action of mitochondrial dehydrogenases, forming purple formazan crystals. After incubation, these crystals were dissolved in 2 mL HCl/isopropanol solution (1:24 v/v). The absorbance of the dissolved crystal solution was measured using a spectrophotometer at 620 nm (Cecil Instruments, Cambridge, UK) and compared to a standard absorbance curve to give an approximate cell number.

3. Results

3.1 ASPN-treated UHMWPE

3.1.1 Surface composition

Table 1 lists the compositions of the untreated UHMWPE and ASPN-treated UHMWPE surfaces as measured using XPS, whilst Fig. 3(a) shows the N:C and O:C ratios as a function of treatment time. These results show that the ASPN treatment is effective in incorporating nitrogen-containing moieties at the UHMWPE surface after a treatment time of 10 min. It can also be seen that increasing the ASPN treatment time to 30 min yields a further increase in the N:C ratio. The compositions of the 30 min and 60 min ASPN-treated samples are similar, and the treatment can therefore be considered to have reached equilibrium after 60 min. A detailed analysis of the deconvolution of the C 1s, N 1s and O 1s photoelectron peaks can be found in the Supporting Information.

In summary, the results show that the nitrogen in the plasma has become incorporated into the UHMWPE surfaces in the form of nitrogen-containing groups. The likely groups are C-N and C=N, evidenced by the centre of the N 1s photoelectron peak being located in the binding energy range 399.5-400.0 eV [23,24]Furthermore, the C 1s photoelectron data is suggestive of bonds such as C≡N and N-C-O which would exhibit higher binding energies for the N 1s photoelectron data. However, the N 1s photoelectron peak can only be deconvoluted to give one symmetrical peak.

There are also a number of oxygen-containing groups present in the ASPN-treated UHMWPE which were not present in the untreated UHMWPE. Functionalisation occurs due to chain scission, which promotes the formation of free radicals during ASPN treatment [25]. The bonds identified were in-keeping with the results reported for plasma immersion ion implantation of UHMWPE [26], ammonia pulsed plasma treatment of polymers including poly(propylene) [27-28], and nitrogen plasma treatment of poly(ethylene terephthalate) [23]. Table 2 lists the chemical bond assignments following peak deconvolution [26-31].

Fig. 3(b)-(d) shows the composition of ASPN-treated UHMWPE surfaces stored in air for 28 days; samples were tested on Days 1, 7, 14, 21 and 28 post-treatment. Storage in air did not greatly affect the composition of ASPN10, but there was a small increase in the O:C ratio and decrease in the N:C ratio for ASPN30 and ASPN60, which is suggestive of either oxidation or hydrolysis. Examination of the XPS spectra showed a gradual increase in binding energy of the C 1s photoelectron peaks associated with those chemical bonds which were not C-C. Grace and Gerenser discussed the time-dependent hydrolysis of imine moieties on plasma-treated poly(ethylene) stored in air [31], and it may be that a similar process is occurring here. The C 1s, N 1s and O 1s photoelectron spectra are presented in the Supporting Information.

Table 1. Composition of untreated UHMWPE and ASPN-treated UHMWPE surfaces stored under air for < 24 h as measured by XPS

	Untreated	**ASPN10**	**ASPN30**	**ASPN60**
atomic % C	91.6	61.4	55.1	56.2
atomic % N	0	8.4	35.8	34.2
atomic % O	8.4	30.2	9.1	9.6

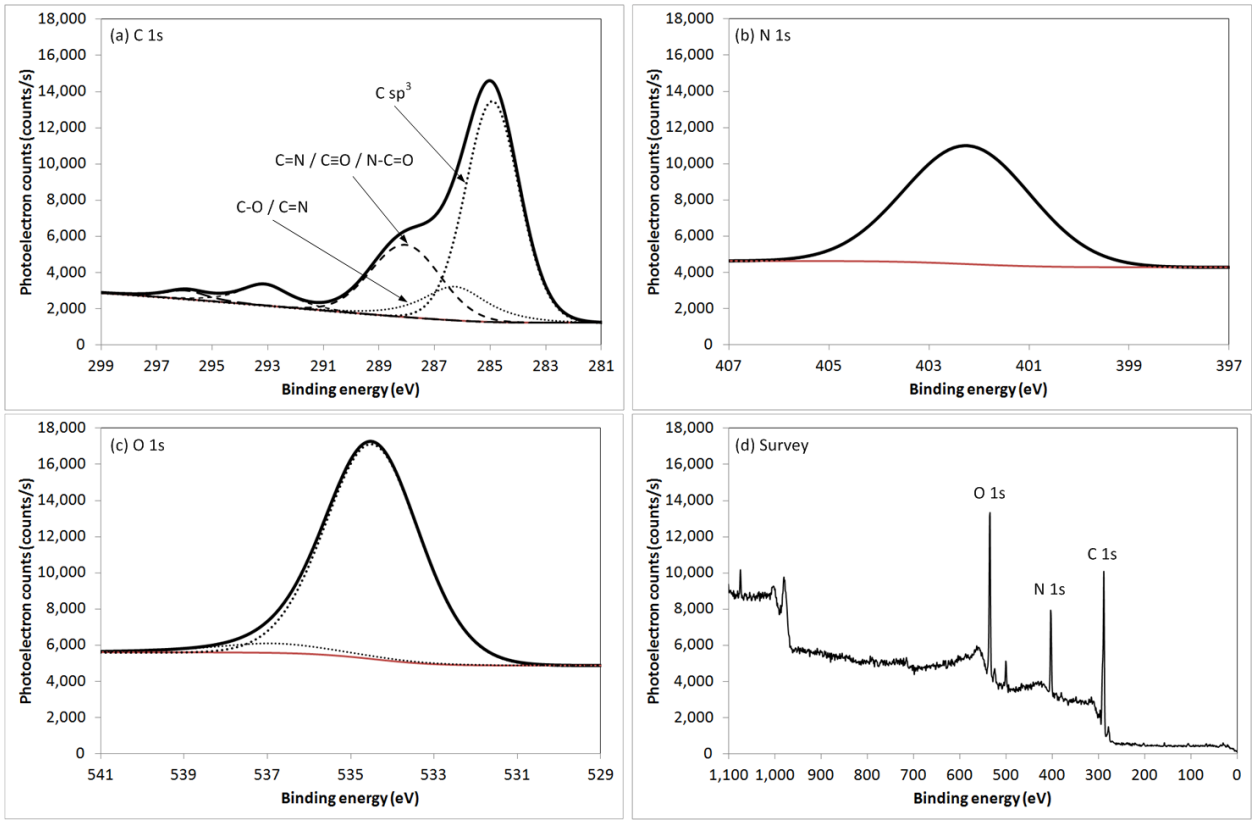

Figure 2. XPS analysis of ASPN60; (a) C 1s photoelectron peak deconvolution, (b) N 1s photoelectron peak deconvolution, (c) O 1s photoelectron peak deconvolution, (d) Survey spectrum showing C 1s, N 1s and O 1s photoelectron peaks

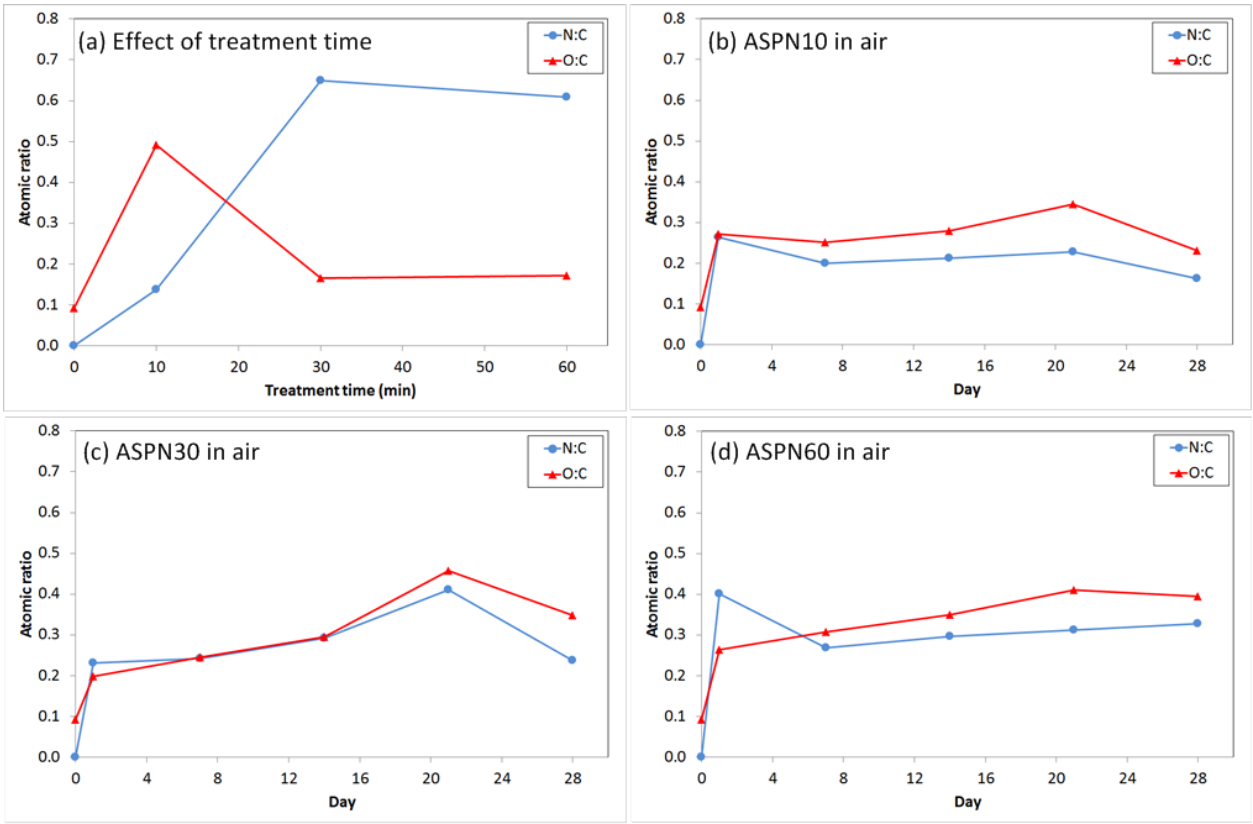

Figure 3. N:C and O:C ratios as a function of treatment time for (a) ASPN-treated UHMWPE surfaces stored in air for < 24 h, (b) ASPN10 stored in air for 28 days, (c) ASPN30 stored in air for 28 days, (d) ASPN60 stored in air for 28 days

Table 2. Peak binding energy (eV) and chemical bond assignment following deconvolution of XPS spectra for untreated UHMWPE and ASPN-treated UHMWPE surfaces stored under air for < 24 h

	Untreated	**ASPN10**	**ASPN30**	**ASPN60**
C 1s	285.1, C-C 287.1, C=O	285.1, C-C 286.9, C-O / C=N 288.3, C=O/ C≡N/ N-C-O	285.0, C-C 286.6, C-O / C=N 288.2, C=O/ C≡N/ N-C-O 293.1, O-C=O	285.0, C-C 286.3, C-O / C=N 288.1, C=O/ C≡N/ N-C-O 293.1, O-C=O
N 1s		400.0, C-N / C=N	399.7, C-N / C=N	399.6, C-N / C=N
O 1s	532.3, C-O	532.1, C-O	531.8, C-O	531.8, C-O 534.8, O=C-O

3.1.2 Surface topography

Topographical analysis of untreated UHMWPE and ASPN-treated UHMWPE revealed that there was no discernible change in surface structure due to the ASPN treatment. Untreated UHMWPE exhibited a mean S_a of 720 ± 100 nm. Fig. 4 shows the topography of the untreated UHMWPE surface over an area of 860 x 640 µm; the height scale is 14 µm. Fig. SI25 in the Supporting Information shows the measured S_a values for ASPN10, ASPN30 and ASPN60 stored (a) in air, (b) under PBS, and (c) under S-DMEM.

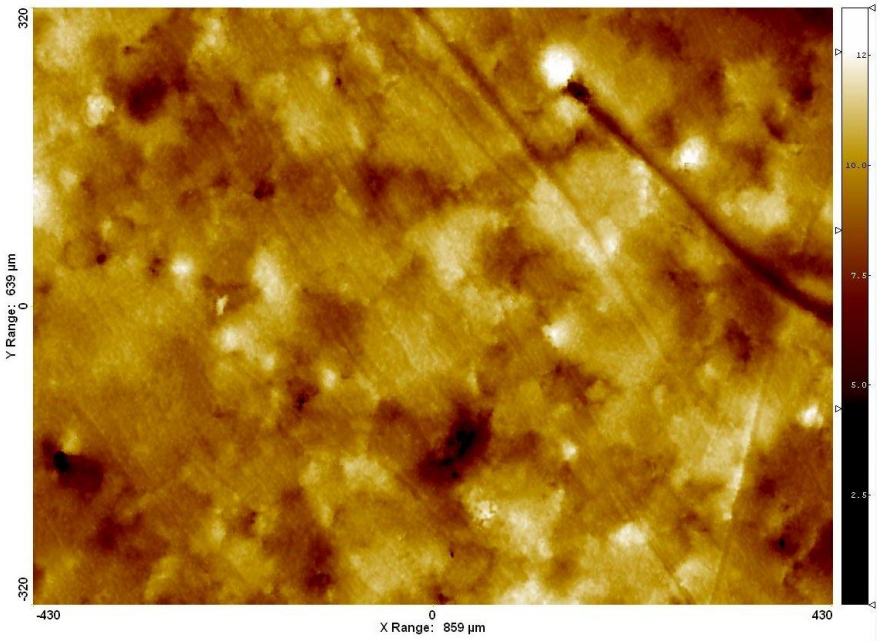

Figure 4. Surface topography of untreated UHMWPE, image dimensions 432 x 321 µm^2

3.1.3 Mechanical properties

Untreated UHMWPE exhibited a reduced modulus of 1.3 ± 0.1 GPa and a hardness of 61 ± 5 MPa, as measured by nanoindentation. The ASPN treatment did not significantly affect the mechanical properties of the UHMWPE surface; all samples exhibited mean reduced moduli in the range 1.0-1.8 GPa and mean hardnesses in the range 50-90 MPa. These results are shown in Fig. 5. The range of variation in the results is not systematic, and is most likely due to local differences in contact area between indenter and sample surface.

3.1.4 Adhesive properties

Adhesion force results are presented as values of F_{peak}/R, where F_{peak} is the maximum adhesive force during probe retraction, and R is the radius of the SiO_2 colloid probe, which for the measurements presented here is 6 μm. Untreated UHMWPE exhibited a mean adhesion force of 51 ± 4 mN/m. Fig. 5 shows the results of AFM measurements of the adhesive properties of ASPN-treated UHMWPE samples. It can be seen that the ASPN treatment left the UHMWPE surface with a residual cationic electrostatic charge, as evidenced in Fig. 5(a) and also in Fig. 5(d), where for ASPN60 on Day 0, a long-range attractive force deflects the AFM cantilever towards the sample surface, even when out of contact. This effect was also observed for ASPN10 and ASPN30 in air on Day 0. By Day 7 the electrostatic attraction had dissipated for all samples in air, leaving a residual adhesion behaviour of a similar magnitude to untreated UHMWPE. ASPN-treated samples stored in PBS did not exhibit any electrostatic attraction on Day 0, and the adhesion behaviour was of a similar magnitude to untreated UHMWPE. In comparison, ASPN-treated samples stored in S-DMEM exhibited greater adhesion than samples stored in PBS and samples stored in air after the electrostatic attraction had dissipated. This result is ascribed to the adsorption of proteins from the S-DMEM solution onto the ASPN-treated sample surface, a process enhanced by the residual cationic charge present upon immersion of the sample into solution.

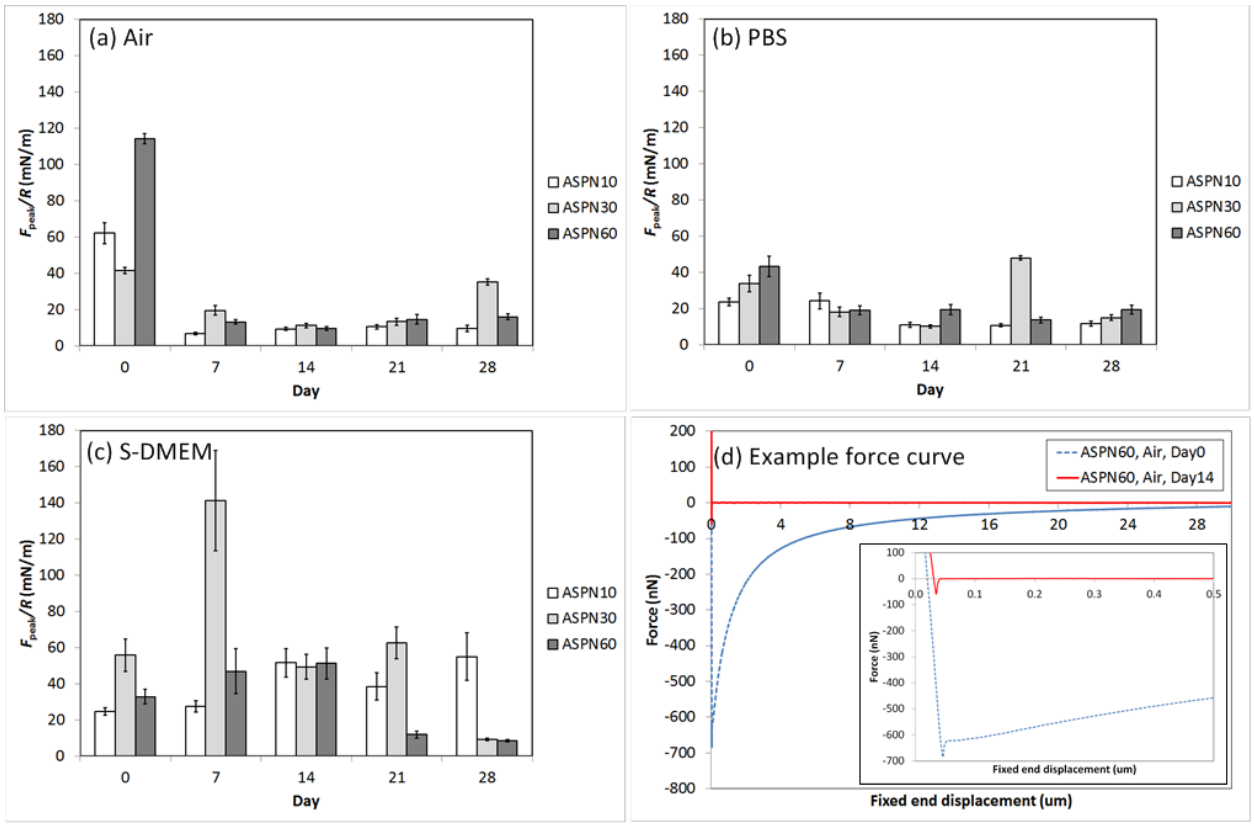

Figure 5. Peak adhesion force for ASPN-treated UHMWPE stored in (a) Air, (b) PBS, and (c) S-DMEM. Example force curves are shown in (d) for ASPN60 stored in air on Day 0 and Day 14; greater detail on the pull-off event can be seen inset.

3.2 Fibroblast culture on ASPN-treated UHMWPE

3.2.1 Scanning electron microscopy

Fig. 6 shows SEM images of the surfaces of (a) untreated UHMWPE and (b-d) ASPN-treated UHMWPE. The images show that fibroblasts do not attach to untreated UHMWPE but respond favourably to the ASPN-treated UHMWPE, with significant deposition of extracellular matrix (ECM) during the three hours post-seeding, leading to well-developed interconnecting material between cells. Treatment time appeared to have little influence on the extent of cell attachment, with ASPN10, ASPN30 and ASPN60 each covered with several layers of fibroblasts.

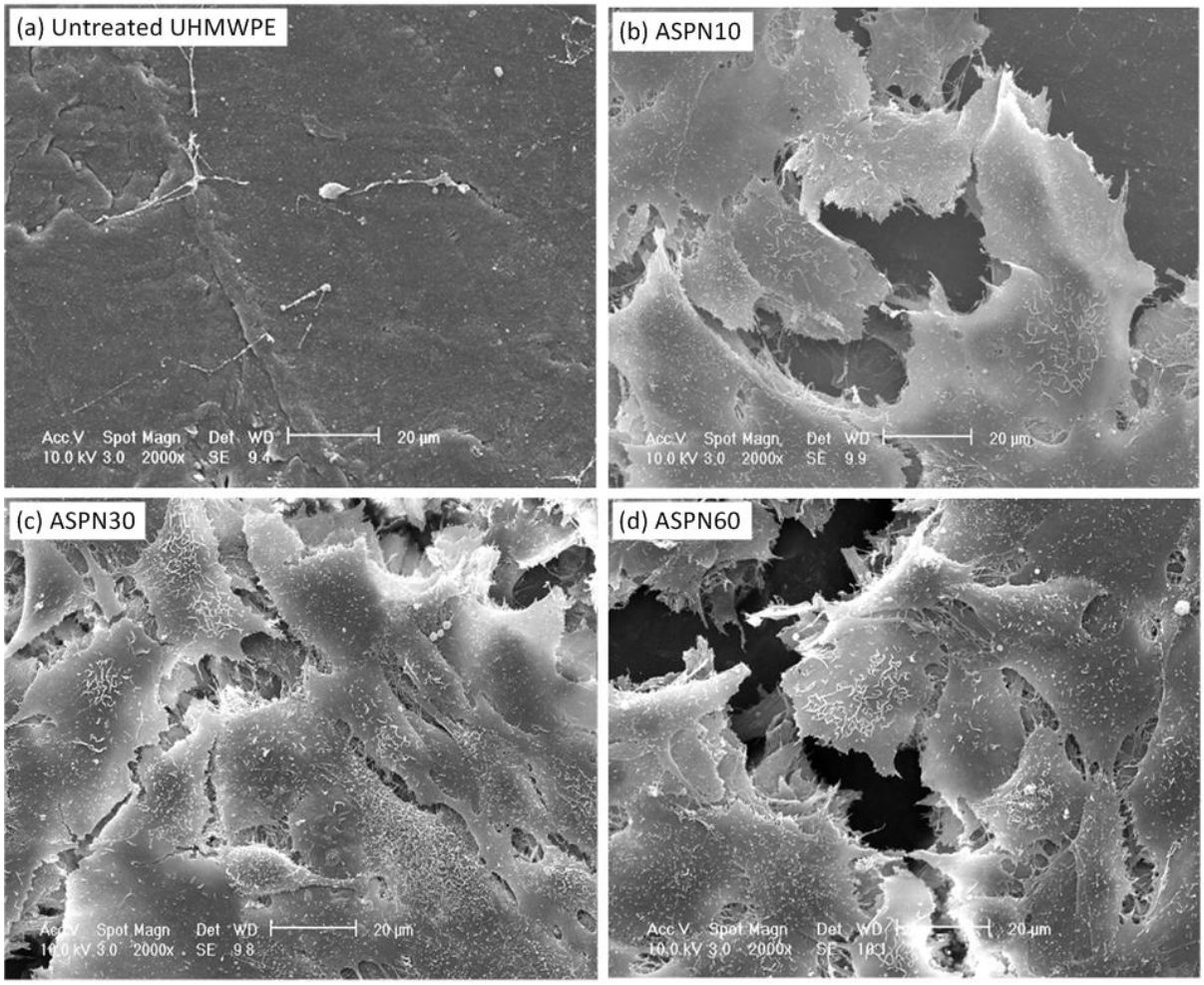

Figure 6. SEM images of fibroblast-seeded surfaces: (a) Untreated UHMWPE, (b) ASPN10 on Day 1, (c) ASPN30 on Day 1, and (d) ASPN60 on Day 1

Fig. 7 shows SEM images of the fibroblast-seeded ASPN60 surface over a period of 28 days. The development of the morphology of the fibroblast layer can be discerned from these images. On Day 0 the surface is covered by a multilayer of cells, but the outline of individual cells can be still observed in some regions. By Day 7, ECM has increased the extent of connective material present between the fibroblasts. By Day 21 and Day 28 there is a well-developed multilayer of fibroblasts, which appears to be flatter and more uniform than the cell layer present on Day 0 and Day 7. The surface topography of the fibroblast layer is reported in §3.2.2.

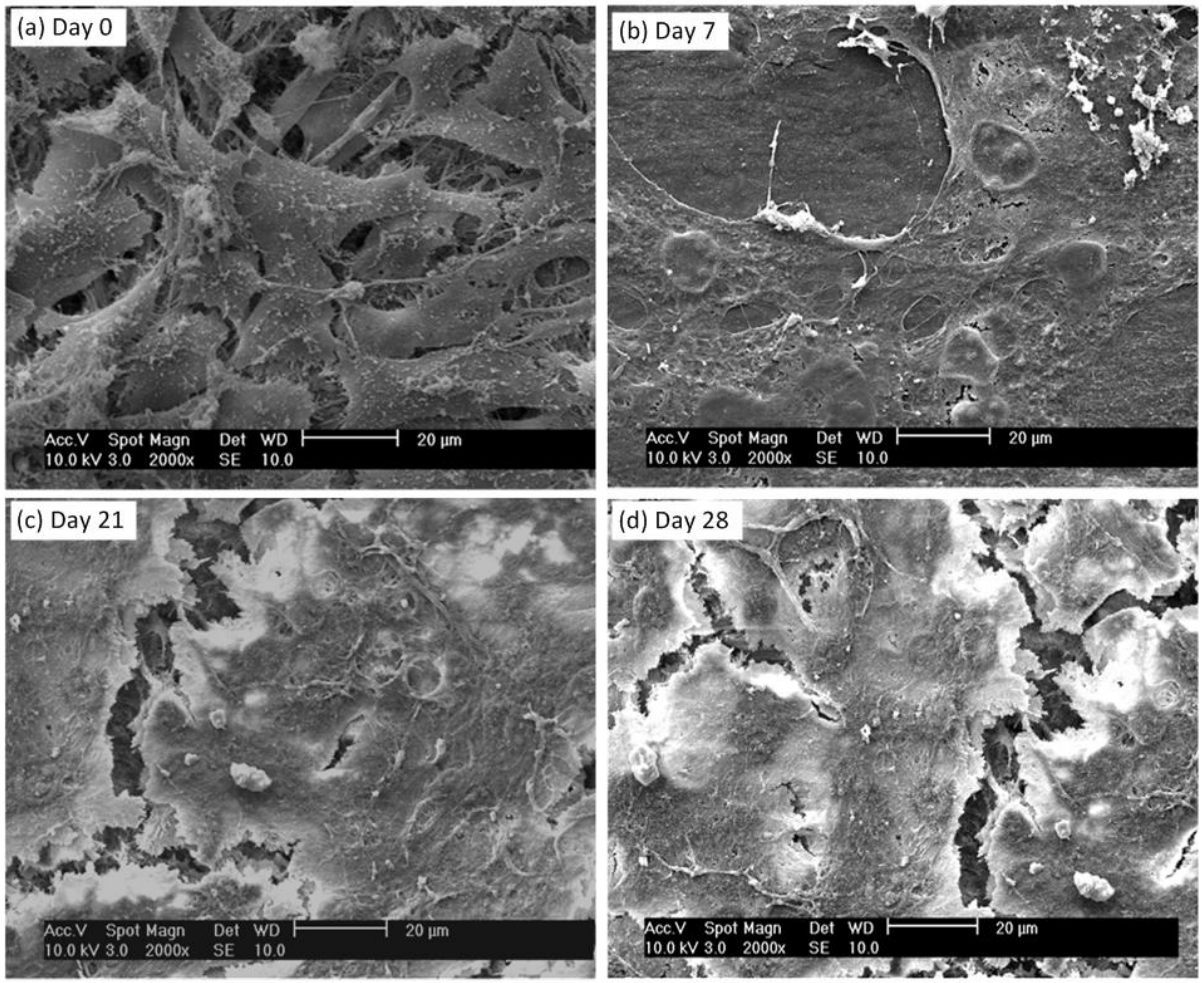

Figure 7. SEM images of fibroblast-seeded ASPN60 on (a) Day 0, (b) Day 7, (c) Day 21, and (d) Day 28

3.2.2 Surface topography

Fig. 8 shows (a-c) the change in surface topography of fibroblast multilayers seeded on ASPN60 over a 28 day period, and (d) typical surface profiles on Days 0, 14 and 28. On Day 0, individual fibroblasts are easily distinguishable and exhibit a rounded morphology punctuated with thin connective extensions between cells. On Day 14 the round cell bodies can still be visualised protruding slightly out of the upper layer. In some regions the connective tissue can be seen also. On Day 28 it is just possible to observe the round cell bodies in the upper layer, but there is now no evidence of connective tissue. Instead, the ECM is now extensive and surrounds the cell in a continuous mass of tissue. The surface profiles reaffirm the discrete nature of the cells on Day 0, and the incorporation of individual cells into layers over the 28 days studied here. Quantitative analysis of multilayer thicknesses showed that on Day 0 the cell layers exhibited a thickness of 18 µm. As the multilayer development progressed, the thickness decreased to 14 µm by Day 7, which remained approximately constant until Day 21. By Day 28 the thickness was 12 µm. The decrease in thickness suggests a gradual contraction of the cells within the multilayer structure over the 28 day period.

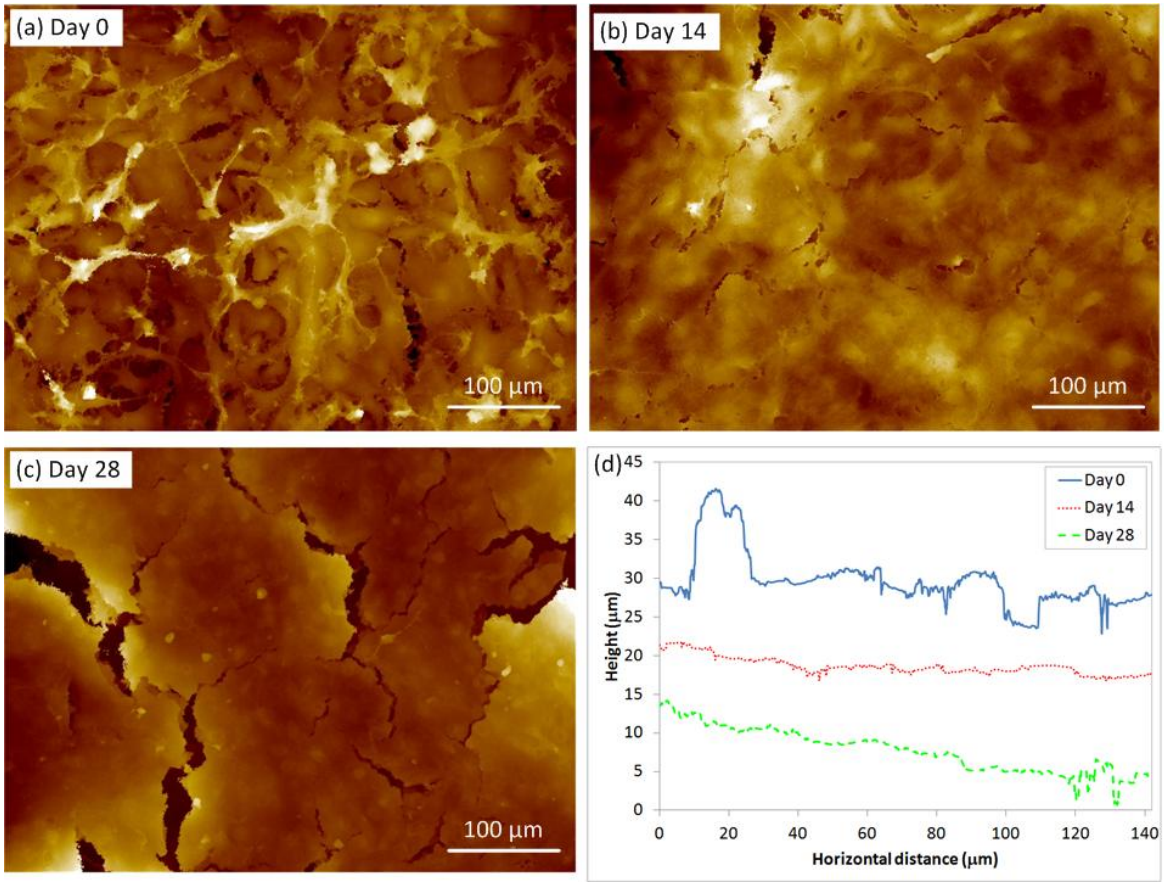

Figure 8. Topography of fibroblast-seeded ASPN60 on (a) Day 0, (b) Day 14, (c) Day 28, and (d) surface profiles; image height scale is 20 µm, image dimensions 432 x 321 μm^2

3.2.3 Atomic force microscopy

Fig. 9 shows the multilayer fibroblast network seeded and developed on ASPN60 on (a) Day 0 and (b) Day 7, in which the connective extensions between cells can clearly be seen. During the force scan mapping imaging, the cells supported compressive loading of 5 nN, although the cells did move downwards slightly in response to the applied load. This compliance during loading suggested that the connections between cells were under tensile stress. The adhesion force between the SiO_2 cantilever tip and the fibroblast surface, presented as the peak force divided by the nominal tip radius (F_{peak}/R), increased from 6 ± 1 mN/m on Day 0 to 25± 5 mN/m on Day 7. By Day 14 F_{peak}/R increased to 46 ± 12 mN/m, whilst by Day 28 there was a reduction in F_{peak}/R to 23 ± 5 mN/m. By Day 28 a number of adhesion force curves exhibited the phenomenon of polymer chain pulling, which occurs when surface polymers adhere to the AFM cantilever tip and are stretched and unfolded, until the elastic response of the protein chain is sufficient to overcome the adhesion of the polymer to the tip, whereupon a snap-off event occurs. This phenomenon was not observed on Days 0, 7 or 14. A worm-like-chain (WLC) model [32] was employed to model the persistence length and contour length of these surface polymers (JPK Data Processing software, JPK, Germany) which were calculated as 370 pm and 54 µm, respectively. The polymer chains exhibited a detachment force of the order of 140 pN.

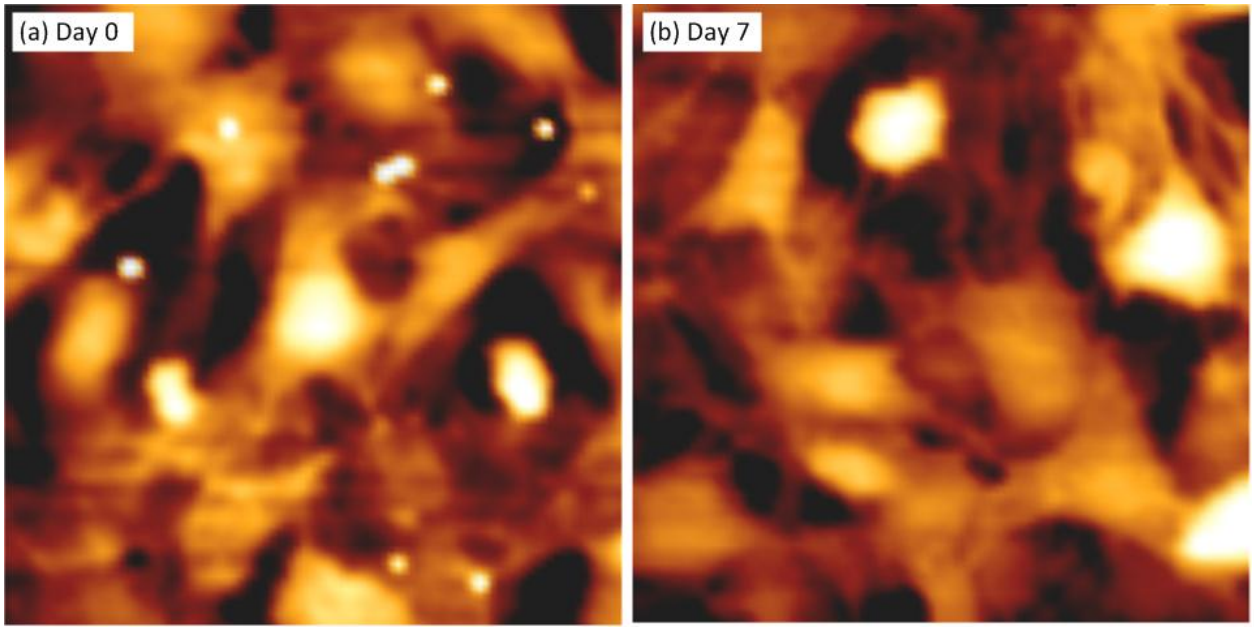

Figure 9. AFM images of fibroblast-seeded ASPN60 on (a) Day 0, and (b) Day 7; image height scale is 15 µm

3.2.4 Metabolic activity

Fig. 10 shows the results of the MTT metabolic activity essay performed on ASPN60 seeded with fibroblasts on Days 0, 7, 14 and 28 post-seeding. The results show that the fibroblasts metabolic activity was at a maximum on Day 7, with approximately 10^7 cells present on the sample surface. In contrast, this value fell to approximately $3x10^6$ cells by Day 14 and further on to Day 28. However, the samples were initially seeded with $7.5x10^5$ cells, and hence these values suggest that cells were viable on the ASPN60 surface. It was not possible to obtain MTT data for fibroblast-seeded untreated UHMWPE, as a comparison for the ASPN60, because fibroblasts did not adhere to the untreated UHMWPE surface.

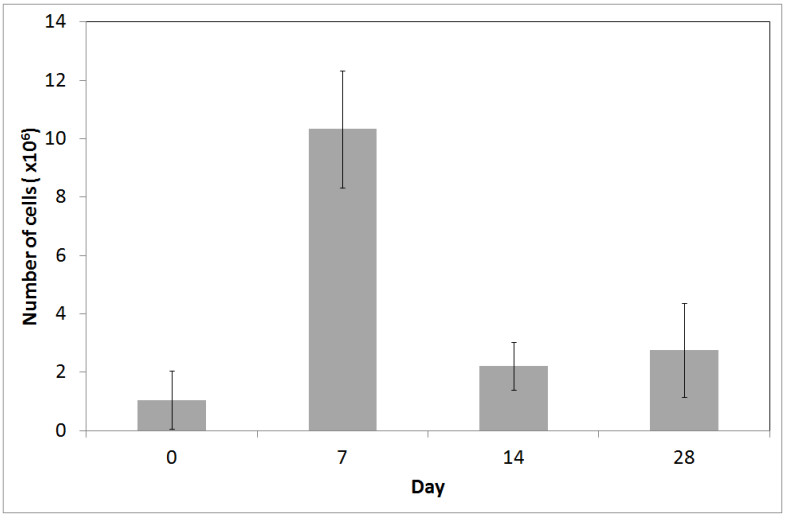

Figure 10. MTT metabolic activity assay performed on fibroblast-seeded ASPN60

4. Discussion

4.1 Effect of ASPN treatment on UHMWPE surface

XPS analysis of the ASPN-treated surface showed that nitrogen-containing groups were incorporated onto the polymer surface, likely in the form of amine moieties, due to the reductive potential of the H_2 content of the N_2/H_2 plasma. The C 1s and N 1s photoelectron peaks suggest that there are C-N covalent bonds formed as a result of the ASPN treatment. In addition to C-N bonds, the C 1s photoelectron peaks suggest that a variety of C-O bonds are formed as a result of the ASPN treatment, such as C−O−C, C=O and O−C=O. It has been reported that UHMWPE may contain peroxides formed during the processing of the polymer to sheets during which free radicals can form along the polymers chains leading to oxidation of the surface [33]. Such linkages and intense peaks are possibly associated with an exposure to air that in the presence of free radicals results in time-dependent oxidation. Oxygen absorption which results in oxidation on the polymer surface is also likely due to the increased functionality of the material with the plasma treatment [34]. It has been reported as a common phenomenon that on polymeric surfaces after a non-oxygen plasma treatment, there is incorporation of oxygen. The reason is that during the nitrogen plasma treatment, free radicals are created on the polymer surface, which react with oxygen, and also remaining free radicals post–treatment react with oxygen when exposed to the atmosphere. Post plasma reactions (post plasma functionalisation) occur because of the fact that the species generated during the treatment are unstable and thus readily react [25,35]. Vesel et al. have treated PTFE with nitrogen plasma and 10 min after the treatment, in addition to nitrogen containing groups, they detected an increased oxygen concentration on the polymer surface [36]. Also Arefi-Khonsari et al. attribute the presence of oxygen on the surface to either (i) the surface oxidation in the plasma chamber due to residual air, or (ii) to post oxidation after the exposure of the sample to ambient air. These processes interfere with the incorporation of nitrogen species into the surface because of the competition of the active sites by oxygen species [28]. It has been reported by Junkar et al., who treated polymers with nitrogen plasma, that the concentrations of nitrogen and oxygen increased following short duration treatments of only 3 s, thus surface saturation with these elements was completed within this duration and further treatment did not affect chemically the materials surface [37]. Also Dekker et al. have treated PTFE surfaces with nitrogen and oxygen plasma, and they found that nitrogen and oxygen incorporation was detected in both treatments. This is attributed to a reaction of nitrogen and oxygen that exist in atmospheric air with long-living polymer radicals, formed during the treatment. Also in this case it is believed that molecular oxygen is more reactive compared to molecular nitrogen. This could explain the oxygen content of the surfaces treated with nitrogen plasma [38].

The hardness and reduced modulus of the UHMWPE surface were not significantly affected by the ASPN treatment, regardless of the treatment duration. These results contrast with the findings of a previous study where the H_2:N_2 ratio in the plasma was 75:25 [21], as opposed to the 20:80 ratio used here. The 75:25 ASPN-treated UHMWPE surface was previously found to exhibit a higher hardness and reduced modulus than the untreated UHMWPE. This finding is in-keeping with the results reported by Toth *et al*. [39] who measured a larger modulus, hardness, and scratch resistance for H_2-treated UHMWPE. Therefore, the UHMWPE surface mechanical properties can be tailored through careful selection of the H_2:N_2 ratio employed during ASPN treatment.

The topography of the UHMWPE surface was also not significantly affected by the ASPN treatment, regardless of the treatment duration. This is in contrast with results presented by Chu *et al*. [15] and Silva *et al*. [40] in which plasma treatments resulted in an increased polymer surface roughness on the nanoscale. However, the lateral dimensions of the seeded fibroblasts meant that the analysis area considered in this work is much larger than considered by Chu *et al*. or Silva *et al*., because of which the initial surface roughness measured is of sufficient magnitude that a nanoscale change in roughness would be imperceptible.

4.2 Effect of storage on ASPN-treated UHMWPE

There was no discernible change in the surface topography or mechanical properties of ASPN-treated UHMWPE over the 28 day period studied, for all three storage environments. AFM analysis of ASPN-treated UHMWPE stored in air revealed that the electrostatic adhesion properties of the surface decreased between Day 0 and Day 7, and then remained approximately constant up to Day 28. In contrast, ASPN-treated UHMWPE stored under aqueous solutions exhibited smaller adhesion forces than ASPN-treated UHMWPE stored in air. This result suggested that residual electrostatic charges remaining in the sample following the ASPN treatment were rapidly dissipated by the surrounding liquid environment on Day 0. Therefore, electrostatic forces are unlikely to have influenced the cell attachment process.

4.3 Attachment of fibroblasts to ASPN-treated UHMWPE

The morphology of fibroblasts attached to ASPN-treated UHMWPE was observed to be similar regardless of the treatment duration, as shown in Fig. 6. Therefore ASPN60 was used to evaluate the time-dependent behaviour of fibroblasts on the ASPN-treated UHMWPE surface. Observation on Day 0 by SEM and interferometry revealed that fibroblasts were interconnected and exhibited an ellipsoidal shape. Cytoplasmic extensions were observed and the filopodia of adjacent fibroblasts were conjoined. These results are shown in Figs. 6-7. A distinctive change in the morphology of the fibroblast layer was observed between Day 0 and Day 7 onwards, whereby the surface layer is flattened and individual fibroblasts could no longer be easily distinguished. The thickness of the fibroblast layer decreased from 18 μm on Day 0 to 12 μm on Day 28. This phenomenon can be explained by the propensity of the fibroblasts to increase their area of contact with the underlying ASPN-treated UHMWPE surface, and also to decrease the void volume between neighbouring fibroblasts. Such a result appears reasonable given that there will be a maximum possible rate of diffusion of nutrients into the layers from the solution, and this may set an upper bound on the total possible number of layers which can be viably maintained as the fibroblasts grow and develop, requiring increased levels of nutrients as they do so.

Generally, cells do not attach to inert surfaces. Adhesion is often preceded by the adsorption of proteins on the material surface, and it is these proteins which are recognized by integrin receptors on the cell membrane which mediate cell attachment. *In vitro* cell attachment on surfaces is mediated by the glycoproteins fibronectin and vitronectin, and it has previously been reported that surfaces presenting amine moieties encourage glycoprotein adsorption, and enhance cell attachment [41-42]. Hence, it is suggested that the amine groups formed on the surface of the ASPN-treated UHMWPE is the reason that fibroblasts attached to the polymer surfaces.

The MTT assay showed a pronounced peak in metabolic activity on Day 7, which indicates that fibroblast proliferation was far in excess of that exhibited on Day 0. The decrease in metabolic activity recorded on Day 14 onwards may be explained by the confluency of the cells on the sample surface. i.e. Fibroblasts occupy all of the available surface area, as evidenced by the SEM images in Fig. 7, particularly Fig. 7(b). Upon reaching full confluency, the fibroblast metabolic activity decreases substantially, seemingly due to contact inhibition, a property introduced to the NIH 3T3 cell line in order to prevent apoptosis, or cell death, once cells are in contact with each other [43].

4.4 Influence of specific chemical moieties on cellular attachment and proliferation

For the purpose of this study it was not possible to examine oxygen plasma treatment, nor was it possible to prevent some oxygen-containing groups forming on the nitrogen plasma-treated surface, a result which is in agreement with

previously reported studies [44-46]. Therefore it cannot be stated definitively if it is the presence of oxygen-containing moieties, nitrogen-containing moieties, or both due to which the observed cell behaviour was favoured. Separating the effect of surface energy changes from the incorporation of specific chemical moieties in a surface is non-trivial. In addition, different cell types have been reported to respond to different surface chemical moieties. In general, contact, attachment and proliferation of cells onto a substrate are time-dependent procedures [47] in which cell adhesion and spreading are phenomena that occur by a series of events and are mediated by the ECM proteins, the integrins [48]. Here we attempt to provide a brief overview of some of the research which has been reported that relates exclusively to oxygen-containing moieties and nitrogen-containing moieties.

4.4.1 Oxygen-containing moieties

Ramsey et al. reported the oxygen plasma treatment of a poly(styrene) surface, in which the treatment increased the surface energy of the polymer and hence the incorporation of oxygen-containing groups enhanced the growth of kidney cells [49]. Ertel et al. reported an increase in the growth of bovine cells on poly(styrene) surfaces which were plasma treated to modify the oxygen content of the surface. It was also found that increasing the oxygen content corresponded to increasing cell growth. This was suggested to be due to the presence of ketone moieties, whilst the presence of hydroxyl and carboxyl groups did not have any influence on cells growth [50].

Plasma discharge modification has been applied to poly(ethylene), poly(tetrafluoroethylene), poly(ethylene terephtalate), poly(styrene) and poly(propylene) surfaces in order to study the effect of the treatment on cell adhesion. Seeding of L-murine fibroblasts on these treated and untreated polymer surfaces yielded a general improvement of cell attachment. This effect was related to (i) increases in surface roughness, and (ii) the generation of chemical moieties such as carboxyl groups after the treatment [51].

4.4.2 Nitrogen-containing moieties

Schroder et al. reported that surface modification in the presence of ammonia plasma improves fibronectin adsorption to the poly(ether ethyl ketone) surface, which consequently improved the attachment of human osteoblasts; the improved attachment was solely attributed to the presence of amino moieties that were introduced during the plasma treatment [52]. Tseng et al. reported that expanded poly(tetrafluoroethylene) vascular grafts treated with radio frequency glow discharge in amide and amine plasma incorporated nitrogen groups in the polymer surface and also led to enhanced hydrophilicity. Endothelial cell seeding onto the plasma treated surfaces revealed that the modified polymer was a better substrate for endothelial cell attachment when compared to the untreated polymer [53]. Additionally, Ho et al. investigated the effect of nitrogen plasma on the UHMWPE surface, and the results showed clearly that the treatment enhanced protein retention compared to the untreated UHMWPE [54]. Poly(ethylene terephthalate) surfaces have been treated with NH_3, NH_3/H_2, O_2/H_2 and O_2/H_2O plasmas. On the plasma treated surfaces, endothelial cells isolated from the human umbilical cord vein were seeded for incubation periods of between 2-9 days. On the plasma treated surfaces, cell proliferation was shown to be improved in comparison to the untreated surfaces. Moreover, the nitrogen-containing plasma-treated surfaces proved to be the best substrates for endothelial cell proliferation compared to surfaces that were treated exclusively with oxygen or hydrogen plasma [55].

5. Conclusions

Active screen plasma nitriding (ASPN) has been used to modify the surface chemistry of UHMWPE without altering the mechanical properties and topography of the polymer surface. ASPN was found to incorporate amine groups into the UHMWPE surface which were stable in air for up to 28 days post-treatment. Furthermore, the amine groups promoted the adhesion and viability of fibroblasts seeded within 24 h of the plasma treatment. The morphology and thickness of the fibroblast layer was monitored for 28 days post-seeding. A 33 % reduction in layer thickness was recorded over the 28 day period studied, as well as a decrease in the roughness of the uppermost layer, as the outline of individual fibroblasts became less discernible.

Acknowledgements

GK would like to thank the EPSRC for the financial support of the present study via a DTA studentship at the School of Metallurgy and Materials, University of Birmingham. The atomic force microscope, nanoindenter and interferometer used in this research were obtained, through Birmingham Science City: Innovative Uses for Advanced Materials in the Modern World (West Midlands Centre for Advanced Materials Project 2), with support from Advantage West Midlands (AWM) and part funded by the European Regional Development Fund (ERDF). The authors acknowledge the excellent assistance with XPS analysis provided by the Leeds EPSRC Nanoscience and Nanotechnology Research Equipment Facility (LENNF), funded by EPSRC Grant EP/F056311/1 and the University of Leeds.

Supporting Information

X-ray photoelectron spectroscopy results of ASPN-treated UHMWPE showing deconvoluted C 1s, N 1s and O 1s photoelectron peaks for ASPN10, ASPN30, ASPN60 within 24 h of treatment, and during storage in air for up to 28 days.

References

1. Y. Ikada Y, Surface modification of polymers for medical applications, Biomaterials 15 (1994) 725-736.
2. B.D. Ratner, Plasma deposition for biomedical applications: A brief review, J. Biomat. Sci. Polym. E, 4 (1992) 3-11.
3. A. Oliva, F.D. Ragione, A. Salerno, V. Riccio, G. Tartaro, A. Cozzolino, S. D'Amato, G. Pontoni, V. Zappia, Biocompatibility studies on glass ionomer cements by primary cultures of human osteoblasts, Biomaterials 17 (1996) 1351-1356.
4. B.D. Ratner, Surface modification of polymers: chemical, biological and surface analytical challenges, Biosens. Bioelectron. 10 (1995) 797-804.
5. W. Shi, X.Y. Li, H. Dong, Improved wear resistance of UHMWPE by plasma immersion ion implantation, Wear, 250 (2001) 544-552.
6. D. Hegemann, H. Brunner, C. Oehr, Plasma treatment of polymers for surface and adhesion improvement, Nucl. Instrum. Meth. B 208 (2003) 281-286.
7. F. Arefi-Khonsari, M. Tatoulian, J. Kurdi, S. Ben-Rejeb, J. Amouroux, Study of the surface properties and stability of polymer films treated by NH_3 plasma and its mixtures. J Photopolym Sci Technol 1998;11:277-292.
8. J.Y. Wong, J.B Leach, X.Q. Brown, Balance of chemistry, topography, and mechanics at the cell-biomaterials interface: Issues and challenges for assessing the role of substrate mechanics on the cell response, Surf. Sci. 570 (2004) 119-133.
9. V.S. Bessmertnyi, Plasma treatment of glasses (a review), Glass Ceram. 58 (2001) 221-224.
10. C.C. Wu, C.I. Wu, J.C. Sturm, A. Kahn, Surface modification of indium tin oxide by plasma treatment: An effective method to improve the efficiency, brightness, and reliability of organic light emitting devices, Appl. Phys. Lett. 70 (1997) 1348-1350.
11. E.M. Liston, L. Martinu, M.R. Wertheimer, Plasma surface modification of polymers for improved adhesion: a critical review, J. Adhesion Sci. Technol. 7 (1993) 1091-1127.
12. J.R. Conrad, J.L. Radtke, R.A. Dodd, F.J. Worzala, N.C. Tran, Plasma source ion-implantation technique for surface modification of materials, J. Appl. Phys. 62 (1987) 4591-4596.
13. H. Chen, G. Belfort, Surface modification of poly(ether sulfone) ultrafiltration membranes by low temperature plasma-induced graft polymerisation, J. Appl. Polym. Sci. 72 (1999) 1699-1711.

14. B.D. Ratner, A. Chilkoti, G.P. Lopez, Plasma deposition and treatment for biomaterial applications. In: R. D'Agostino (Ed). Plasma deposition, treatment, and etching of polymers. San Diego: Academic Press, 1990, pp. 471-510
15. P.K. Chu, J.Y. Chen, L.P. Wang, N. Huang, Plasma-surface modification of biomaterials, Mater. Sci. Eng. 36 (2002) 143-206.
16. J. Georges, US Patent 1999 5,989,363, No. 23.
17. C.X. Li, T. Bell, H. Dong, A study of active screen plasma nitriding, Surf. Eng. 18 (2002) 174-181.
18. C.X. Li, T. Bell, Corrosion properties of active screen plasma nitrided 316 austenitic stainless steel, Corrosion Sci. 46 (2004) 1527-1547.
19. C. Zhao, C.X. Li, H. Dong, T. Bell, Study on the active screen plasma nitriding and its nitriding mechanism, Surf. Coat. Tech. 201 (2006) 2320-2325.
20. S.C. Gallo, H. Dong, New insights into the mechanism of low-temperature active-screen plasma nitriding of austenitic stainless steel, Scripta Mater. 67 (2008) 89-91.
21. G. Kaklamani, N. Mehrban, J. Chen, J. Bowen, H. Dong, L.M. Grover, A. Stamboulis, Effect of plasma surface modification on the biocompatibility of UHMWPE, Biomed. Mater. 5 (2010) 054101.
22. J. Bowen, D. Cheneler, D. Walliman, S.G. Arkless, Z. Zhang, M.C.L. Ward, M.J. Adams, On the calibration of rectangular atomic force microscope cantilevers modified by particle attachment and lamination, Meas. Sci. Technol. 21 (2010) 115106.
23. A. Vesel, M. Mozetic, Modification of PET surface by nitrogen plasma treatment, J. Phys. Conf. Ser. 100 (2008) 012027.
24. G. Beamson, D. Briggs, High resolution XPS of organic polymers: The Scienta ESCA300 database. Wiley, 1992.
25. M.R. Sanchis, O. Calvo, O. Fenollar, D. Garcia, R. Balart, Characterization of the surface changes and the aging effects of low-pressure nitrogen plasma treatment in a polyurethane film, Polym. Test. 27 (2008) 75-83.
26. A.R. Marcondes, M. Ueda, K.G. Kostov, A.F. Beloto, N.F. Leite, Improvements of ultra-high-molecular weight polyethylene mechanical properties by nitrogen plasma immersion ion implantation, Braz. J. Phys. 34 (2004) 1667-1672.
27. I. Gancarz, J. Bryjak, G. Pozniak, W. Tylus W, Plasma modified polymers as a support for enzyme immobilization, Eur. Polym. J. 39 (2003) 2217-2224.
28. F. Arefi-Khonsari, M. Tatoulian, J. Kurdi, S. Ben-Rejeb, J.N. Amouroux, Study of the surface properties and stability of polymer films treated by NH3 plasma and its mixtures, J. Photopolym. Sci. Tech. 11 (1998) 277-292.
29. C. Arpagaous, R. Rohr, Short-time plasma surface modification of HDPE powder in a Plasma Dawner Reactor-process, wettability improvement and ageing effects, Appl. Surf. Sci. 252 (2005) 1581-1595.
30. D.J. Wilson, R.L. Williams, R.C. Pond, Plasma modification of PTFE surfaces, Surf. Interface Anal. 31 (2001) 385-396.
31. J.M. Grace, L.J. Gerenser, Plasma treatment of polymers, J. Disp. Sci. Technol. 24 (2003) 305-341.
32. A. Janshoff, M. Neitzert, Y. Oberdörfer, H. Fuchs, Force spectroscopy of molecular systems - single molecule spectroscopy of polymers and biomolecules, Angew. Chem. Int. Ed. 39 (2000) 3212-3237.
33. S.M. Kurtz, The UHMWPE handbook. Ultra-high molecular weight polyethylene in total joint replacement, Elsevier Academic Press, 2004.
34. N.P. Rhodes, D.J. Wilson, R.L. Williams RL, The effect of gas plasma modification on platelet and contact phase activation processes, Biomaterials 28 (2007) 4561–4570.
35. U. Lommatzsch , D. Pasedag , A. Baalmann, G. Ellighorst, H.E. Wanger, Atmospheric pressure plasma jet treatment of polyethylene surfaces for adhesion improvement. Plasma Process. Polym. 4 (2007) 1041-1045

36. A. Vesel, M. Mozetic, A. Zalar, XPS characterization of PTFE after treatment with RF oxygen and nitrogen plasma. Surf. Interface Anal.40 (2008) 661–663
37. I. Junkar, A. Vesel, U. Cvelbar, M. Mozetic , S. Strnad , Influence of oxygen and nitrogen plasma treatment on polyethylene terephthalate (PET) polymers. Vacuum 84 (2010) 83-85
38. A. Dekker, K. Reitsma, T. Beugeling, A. Bantjes, J. Feijen, W.G. Aken, Adhesion of endothelial cells and adsorption of serum proteins on gas plasma-treated polytetrafluoroethylene. Biomaterials 12 (1991) 130-138
39. A. Toth, M. Mohai, T. Ujvari, I. Bertoti, Hydrogen plasma immersion ion implantation of ultra-high molecular weight polyethylene, Surf. Interface Anal. 38 (2006) 898-902.
40. S.S. Silva, S.M. Luna, M.E. Gones, J. Benesch, I. Pashkuleva, J.F. Mano, R.L. Reis, Plasma surface modification of chitosan membranes characterization and preliminary cell response studies, Macromol. Biosci. 8 (2008) 568–576.
41. H.J. Griesser, R.C. Chatelier, T.R. Gengenbach, G. Johnson, J.G. Steele, Growth of human cells on plasma polymers: putative role of amine and amide groups, J. Biomater. Sci. Polym. Edn. 5 (1994) 531–554.
42. J.G. Steele, G. Johnson, C. McFarland, B.A. Dalton, T.A. Gengenbach, R.C. Chatelier, P.A. Underwood, H.J. Griesser, Roles of serum vitronectin and fibronectin in initial attachment of human vein endothelial cells and dermal fibroblasts on oxygen- and nitrogen-containing surfaces made by radiofrequency plasmas, J. Biomater. Sci. Polym. Edn. 5 (1994) 511–532.
43. R.W. Holley, J.A. Kiernan, "Contact inhibition" of cell division in 3T3 cells, Proc. Nat. Acad. Sci. 60 (1968) 300-304.
44. S. Luna, S. Silva, M.E. Gomes, J.F. Mano, R.L. Reis, Cell adhesion and proliferation onto chitosan-based membranes treated by plasma surface modification. J Biomater Appl 26 (2011) 101-116.
45. I. Junkar, U. Cvelbar, M. Lehicky, Plasma treatment of biomedical materials. Materials and Technology. 3 (2011) 221-226.
46. I. Beaulieu, M. Geissler, J. Mauzeroll, Oxygen plasma treatment of polystyrene and zeonor: substrates for adhesion and pateerned cells, Langmuir, 25 (2009) 7169-7176.
47. P. Parhi, A. Gola, E. Vogler. Role of proteins and water in the initial attachment of mammalian cells to biomedical surfaces: A review. J Adhes Sci Technol. 24 (2010) 853-888.
48. T.G. Kooten, H.T. Spijker, H.J. Busscher. Plasma-treated polystyrene surfaces: model surfaces for studying cell-biomaterial interactions. Biomaterials. 25 (2004) 1735-1747.
49. W.S. Ramsey, W. Hertl, E.D. Nowlan, N.J. Binkowski. Surface treatments and cell attachment. In Vitro. 20 (1983) 802-808.
50. S.I. Ertel, A. Chilkoti, T.A. Horbett, B.D. Ratner. Endothelial cell growth on oxygen-containing films deposited by radio-frequency plasmas: the role of surface carbonyl groups. J Biomater Sci Polymer. 3 (1991) 163-183.
51. Y. Tamada, Y.Ikada. Cell adhesion to plasma-treated polymer surfaces. Polymer. 34 (1993) 2208-2212.
52. K. Schroder, B. Finke, H. Jesswein, F. Luthen, A. Diener. J Adhes Sci Technol. 24 (2010) 905-923.
53. D.Y. Tseng, E.R. Edelman. Effects of amide and amine plasma-treated ePTFE Vascular Grafts on Endothelial Cell Lining in an Artificial Circulatory System. CCC 0021-9304/98/020188-11. 1998 189-198.
54. P.Y.J. Ho, N.J. Nosworthy, M.M.M. Bilek, B.K. Gan, D.R. McKenzie. Plasma Process Polym. 4 (2007) 583-590.
55. P.A. Ramires, L. Mirenghi, A.R. Romano, F. Palumbo, G. Nicolardi. Plasma-treated PET surfaces improve the biocompatibility of human endothelial cells. 2000; John Wiley & Sons, Inc. 535-539.